RSC Advances

PAPER

View Article Online
View Journal | View Issue

CrossMark click for updates

Cite this: RSC Adv., 2015, 5, 23410

High temperature and oil tolerance of surfactant foam/polymer–surfactant foam†

Lin Sun,[a] Wanfen Pu,*[a] Jun Xin,[b] Peng Wei,[a] Bing Wang,[a] Yibo Li[a] and Chengdong Yuan[a]

Received 29th December 2014
Accepted 25th February 2015

DOI: 10.1039/c4ra17216g

www.rsc.org/advances

Foam performance during oil displacement is closely related to the reservoir environment. In this study, both bulk and porous media experiments were conducted to investigate surfactant foam and polymer–surfactant foam behaviors at high temperature and with crude oil. After aging at 90 °C for 90 days, the foam drainage half-life of the aged polymer–surfactant foam was four times longer than that of the fresh surfactant foam. Scanning electron microscope images indicated that, even experienced high temperature aging, the polymer and surfactant could still develop multilayer complexes to enhance the foam film strength. Within a certain oil content, the foam stability in the presence of oil could be better than in the absence of oil. Stereoscopic microscope images revealed that the existing form and content of oil in the foam film had played a vital role. Core flooding experiments further confirmed that stable surfactant foam and polymer–surfactant foam could generate in the presence of waterflooded residual oil and give rise to additional oil recovery of 15.35% and 35.75% at 90 °C, respectively. The positive responses of this study may be attractive to potential foam field applications.

Published on 25 February 2015. Downloaded by Michigan State University on 29/01/2016 16:18:21.

1. Introduction

It is well established that foam flooding is a promising enhance oil recovery method for good mobility control capability and selective blocking features.[1–4] Stable foam is crucial for successful foam flooding. Several methods such as the addition of proper polymers or nanoparticles to surfactant solution are proposed to increase foam stability.[5–8] However, in the oil displacement application, more attention should be given to whether these foams could remain stable in the reservoirs that possess high temperature crude oil.

1.1. Foam in high temperature

Generally, foam has certain stability at high temperature, and even could be used to control mobility for steam flooding.[9,10] However, as temperature increases, foam stability reduces significantly. This could be attributed to multiple factors. First, the stability of foaming surfactant decreases. High temperature would make some foaming surfactants become less water soluble and may precipitate in foam lamellae. If temperature is high enough, the surfactant would decompose, especially when the pH is also improper.[11–13] Second, the diffusion of gas through foam film increases. With increasing temperature, the average energy of gas molecules and the collision frequency of gas molecules with surfactant molecules at the interface increases. Therefore, more gas molecules would overcome the energy barrier and pass through the foam film.[14,15] Third, high temperature changes the microscopic organization of some surfactant molecules in bulk and at the gas/water interface, and decreases the adsorption density of them.[16,17] This might affect capillary drainage and hence foam stability. Four, the viscosity of foam solution decreases with increasing temperature, which would weaken the strength of foam film.[18]

Foam flooding is a time consuming process. It is very important whether the foaming surfactants could maintain their properties for such a long period. Meanwhile, since additives such as polymers are used to enhance foam stability, their performance under high temperature conditions is also worth studying.

1.2. Foam in the presence of oil

The effect of oil on foam property has been a subject of debate for a long time. In the literature, numerous experiments had demonstrated the detrimental effect of oil on foam stability.[19–23] But other studies supported that relatively stable foam could be produced in the presence of oil by selecting proper foam solution. Nikolov *et al.*[24] found that foam stability was enhanced by increasing the hydrophobic chain length of the hydrocarbon surfactants. Li *et al.*[25] observed that the mixture of lauryl betaine and an anionic surfactant blend NI was a good foaming agent

[a]State Key Laboratory of Oil and Gas Geology and Exploitation, South West Petroleum University, Chengdu, Sichuan 610500, China

[b]CNPC Chuanqing Drilling Engineering Company Limited, Geological Exploration and Development Research Institute, Chengdu, Sichuan 610501, China

† Electronic supplementary information (ESI) available: Partial results of the early research on the screening of surfactant foam and polymer–surfactant foam. See DOI: 10.1039/c4ra17216g

This journal is © The Royal Society of Chemistry 2015

Published on 25 February 2015. Downloaded by Michigan State University on 29/01/2016 16:18:21.

with and without the presence of crude oil. Meanwhile, several researchers reported that fluorinated surfactant could generate better oil tolerance foam. Vikingstad[26] found that, in the presence of different types of alkenes, perfluoroalkyl betaine FS-500 formed stable foam as with no oil. Mannhardt *et al.*[27] pointed out that the addition of fluorinated surfactant to various types of hydrocarbon surfactants increased their foam tolerance to oil. Andrianov *et al.*[28] and Cubillos *et al.*[29] documented similar results for the fluorinated surfactants used in experiments.

In order to estimate foam stability in the presence of oil, some parameters such as entering coefficient (E), spreading coefficient (S), lamella number (L) and bridging coefficient (B) were proposed:[30]

$$E = \sigma_{aw} + \sigma_{ow} - \sigma_{oa}$$

$$S = \sigma_{aw} - \sigma_{ow} - \sigma_{oa}$$

$$L = 0.15\sigma_{aw}/\sigma_{ow}$$

$$B = {\sigma_{aw}}^2 + {\sigma_{ow}}^2 - {\sigma_{oa}}^2$$

where σ_{aw} was surface tension between gas and water, σ_{ow} was interfacial tension between oil and water, and σ_{oa} was surface tension between oil and gas. However, foam–oil interaction was a complicated question which was difficult to be explained only by the relationship among different surface (interfacial) tensions. Vikingstad *et al.*[31] reported that spreading coefficient and lamella number could not predict the stability of foam with added oil. The foam stability was strongly dependent on the amount of oil added. Aveyard *et al.*[32] considered that entering coefficient and spreading coefficient could not describe the rate at which oil entering and spreading occurred, thus the foam stability could not be determined. Lee *et al.*[33] demonstrated that the entering, spreading, and bridging coefficients were unable to explain the effects of the type of oil added. They believed that the foam stability in the presence of oil depended on the dispersed oil and the solubilized oil. Between the oil droplet and the gas phase, there was an aqueous film called pseudo-emulsion film. It was widely believed that the pseudo-emulsion film governed the foam stability.[33–35] If the pseudo-emulsion film was stable, the foam could keep stable; on the contrary, if it collapsed, the foam could rupture. However, the stability of pseudo-emulsion film was difficult to accurately measure in real time, and the factors which affected its stability were complicated. Therefore, it remains a challenge to control the stability of pseudo-emulsion film and effectively increase the limiting oil saturation of foam with oil.

The goals of this study are as follows: (1) gain insight into foam behaviors at high temperature and with crude oil, and (2) compare high temperature tolerance, oil tolerance and displacement efficiency of surfactant foam with polymer–surfactant foam. A three-fold approach has been adopted for these objectives. First, the high temperature tolerances of surfactant foam and polymer–surfactant foam were tested by aging experiments. Environment scanning electron microscope (ESEM) was applied to explore the effects of high temperature on the foam microstructures. Then, the foam behaviors in the presence of varying oil content were measured to confirm the oil tolerance of the two foams. The microscopic observations were conducted to determine the key factors which controlled the foam stability in the presence of oil. Finally, the core flooding experiments were performed to investigate the displacement properties of the two foams under high temperature and oil-bearing conditions.

2. Experiment section

2.1. Materials

The surfactants used to perform experiments were sodium dodecyl sulfate (SDS) and imidazoline amphoteric surfactant (LC). The SDS was provided as a solid power by Chengdu Kelong Co., LTD, China (95 wt% active content). The LC was obtained as an aqueous solution from Shanghai XueJie Co., LTD, China (40 wt% active content). This material was water soluble under different pH conditions and produced amphoteric ions when the pH value was around 7. The use concentrations of the SDS and the LC were well above their critical micelle concentration (cmc). The polymer used to conduct experiments was xanthan gum (XG, $M_w = 1 \times 10^7$). It was also supplied as a solid power by Kelong Co., LTD, China (91 wt% active content). The mixture of 0.1 wt% SDS and 0.05 wt% LC which named SL was tested as surfactant foam solution. The mixture of 0.1 wt% SDS, 0.05 wt% LC and 0.15 wt% XG which named SLX was tested as polymer–surfactant foam solution.

The formation water and the crude oil used in experiments were both obtained from an oilfield in China. Salinity and pH of the formation water were 20 813 mg l^{-1} and 7 $\pm$ 0.1. Solutions used in all experiments were prepared with this formation water. Density and viscosity of the crude oil were 0.88 g cm^{-3} at 20 °C and 8.4 mPa s at 90 °C. The composition of the formation water and the crude oil are given in Tables 1 and 2, respectively.

The gas phase used in all bulk and porous media experiments was air. The cores used in porous media experiments were artificial cores which mainly consisted of quartz. These cores were consolidated cuboids and slightly heterogeneous. Their water contact angles of core slice–water–oil system were about 35° which were measured by an optical contact angle measuring instrument (DATAPHYSICS). The main physical properties of the cores are presented in Table 3.

Table 1 Composition of the formation water

Ion	$K^+ + Na^+$	Mg^{2+}	Ca^{2+}	Cl^-	SO_4^{2-}	HCO_3^-
(mg l^{-1})	7797	6	261	12 124	0	610

Table 2 Composition of the crude oil

Component	Saturates	Aromatics	Resin	Asphaltene	Paraffin
(%)	51.21	19.07	29.46	0.26	18.15

Published on 25 February 2015. Downloaded by Michigan State University on 29/01/2016 16:18:21.

Table 3 Physical properties of the core samples used for core flooding

Core number	Cross area (cm^2)	Length (cm)	Porosity (%)	Permeability, K_w (mD)
1#	19.45	31.50	15.01	105.10
2#	19.54	31.50	16.59	105.28
3#	19.57	31.41	16.99	103.57
4#	19.47	31.51	16.23	104.61

The cores were dried to remove the residual water that formed due to the long immersion time in the atmosphere. The dry cores were vacuumed and 100% saturated with formation water. Then their absolute permeability to water (K_w) were measured.

2.2. Bulk foam test setup and procedures

In all bulk foam tests, foams were produced by stirring with a Waring Blender at atmospheric pressure. The foam solution was first heated to 90 °C and then stirred for 1 min at a speed of 4000 rpm to generate foam. A glass cylinder which had a sealing at the top was used to measure the foam volume and then put into a heating oven with temperature of 90 °C. The drainage volume of the foam (that is the volume of the liquid phase below the foam column) was monitored over time through the glass at the front of the heating oven. As the drainage volume of the foam increased, the thickness of the foam films decreased and hence the foam stability weakened.

2.2.1 High temperature tolerance measurements. In order to determine the long term high temperature tolerance of the surfactant foam and polymer–surfactant foam, an aging test was conducted at 90 °C for the corresponding foam solutions. The foam volume and foam drainage half-life of the foam solutions were measured at regular intervals. Every time 200 ml of foam solution was used to generate foam, and the foam drainage half-life was referred to a time when the drainage volume reached 100 ml. Meanwhile, the viscosity variation of the foam solutions was monitored by rotational viscometer (BROOKFIELD) at a shear rate of 7.34 s^{-1} and 90 °C.

ESEM (FEI) was used to survey the microstructures of both fresh and aged foams. First, foams were produced and immediately affixed to a standard copper SEM stub. Second, lyophilization was carried out to prepare freeze-dried foams. Lyophilization is a dehydration process,[36] which could make the foams maintain their original morphology. Next, the foam samples were coated with gold and placed in a specific chamber. Finally, vacuum was applied and the microstructures of the foams could be directly observed through screens.

2.2.2 Oil tolerance measurements. First, foam solution and crude oil were heated to 90 °C separately. Then the crude oil was added to the foam solution before mixing. The foam solution volume was 200 ml, and the added oil volume was calculated as a volume fraction of it. The foam volume and the foam drainage half-life of the mixture were measured. However, the foam drainage half-life here was referred to a time when the drainage volume reached half of the total initial volume of the foam solution and crude oil (that is ≥100 ml). In addition, stereoscopic microscope (ZEISS) was applied to get the microphotographs of foams in the presence of crude oil.

2.3. Core flooding setup and procedures

2.3.1 Core flooding setup. The setup used to conduct the core flooding experiments is shown in Fig. 1. Air-gas was supplied by a 25 MPa cylinder equipped with a pressure regulator. Its flow rate was controlled by a mass flow meter and controller (Bronkhorst). The displacement pump (ISCO) was used to inject formation water, crude oil and foam solutions. The check valves could lead the air and fluids all to flow towards the porous media. The core holder was placed horizontally, and a back pressure valve was connected to the end of it to simulate the formation pressure. The injection fluids, the core holder and the back pressure valve were placed in a heating oven. A data collection system was used to record pressure, liquid production as well as gas and liquid injection rates.

2.3.2 Core flooding procedures. The following steps were included in the core flooding experiments:

(1) All equipment was connected per Fig. 1. The heating oven was set at 90 °C. The back pressure was maintained at 13.7 MPa.

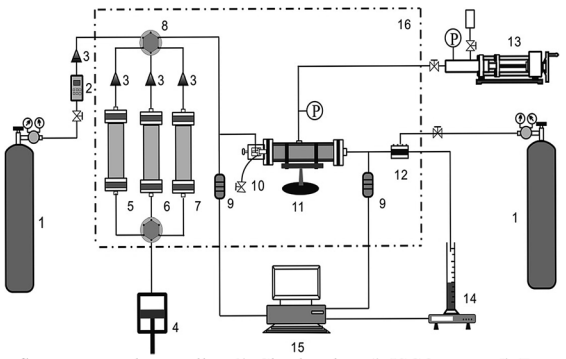

1)-Air supply 2)-Mass flow meter and controller 3)-Check valve 4)-ISCO pump 5)-Formation water 6)-Crude oil 7)-Foam solution 8)-Six-way valve 9)-Pressure transducer 10)-Atmospheric valve 11)-Core holder 12)-Backpressure valve 13)-Manual pump 14)-Production collector 15)-Data collection system 16)-Heating oven

Fig. 1 Schematic of the experimental setup used to perform core flooding experiments.

 This journal is © The Royal Society of Chemistry 2015

Published on 25 February 2015. Downloaded by Michigan State University on 29/01/2016 16:18:21.

Table 4 The displacement agents used between twice water flooding

Core number	Initial oil saturation (%)	Displacement agent
1#	65.22	Air + fresh polymer–surfactant foam solution SLX
2#	64.76	Fresh polymer–surfactant foam solution SLX
3#	65.29	Air + fresh surfactant foam solution SL
4#	63.08	Air + aged polymer–surfactant foam solution SLX (aged at 90 °C for 90 days)

(2) Crude oil was injected at 0.5 ml min^{-1} (from left to right) to form the initial oil. Then the crude oil and the core were equilibrated for 2 days.

(3) Water flooding was performed by injecting formation water at 0.5 ml min^{-1} (corresponding to a true velocity of 2 m per day) until the water cut reached 98%. Water cut is defined as the volume fraction of water in the total liquid production which was produced in 5 minutes.

(4) Air and foam solution were co-injected to carry out foam flooding. The injection rates of air and foam solution were 0.5 ml min^{-1} and 0.25 ml min^{-1}, respectively. The total injection volume was 0.4 PV. Moreover, in order to determine whether the foams were generated in the porous media, 0.4 PV of single polymer–surfactant foam solution was injected (corresponding to polymer–surfactant flooding) at 0.75 ml min^{-1} to compare the oil recovery. The displacement agents used in each core flooding are tabulated in Table 4.

(5) Subsequent water flooding was performed in the same way as the first water flooding until the water cut reached 98% once again.

3. Results and discussion

3.1. High temperature tolerance of foam

On the basis of earlier work, SL (0.1 wt% SDS + 0.05 wt% LC) and SLX (0.1 wt% SDS + 0.05 wt% LC + 0.15 wt% XG) were the most satisfying surfactant foam solution and polymer–surfactant foam solution under the research conditions, respectively. Here, the two foam solutions were aged at 90 °C to determine their long term high temperature tolerance. Fig. 2 shows the changes of their foam volume and foam drainage half-life during aging test.

The initial properties of the SL foam (surfactant foam) and the SLX foam (polymer–surfactant foam) at 90 °C had obvious differences. The former possessed larger foam volume, the latter owned longer foam drainage half-life which was 8.6 times as long as that of the former. It revealed that the XG was unfavorable for foaming, but would effectively improve foam stability. The XG was a kind of semi-rigid polyanion which had glucose units. It hardly modified the surface tension of foam solution (the surface tensions of the SL solution and the SLX solution were 27.4 mN m^{-1} and 27.8 mN m^{-1}, respectively), but could enhance the steric hindrance at the gas/water interface and increase the viscosity and thickness of the foam film.[6,37] Therefore, the liquid drainage rate reduced and the permeation of gas through foam film weakened. Whereas, the increased solution viscosity (the initial viscosities of the SL solution and the SLX solution at 90 °C were 0.5 mPa s and 28 mPa s, respectively) caused the viscous resistance of foaming to rise. Consequently, the foam volume of the SLX foam was 120 ml less than the SL foam.

The changes in properties of the SL foam and the SLX foam during aging were also different. Aged at 90 °C for 90 days, the foam volume and the foam drainage half-life of the SL foam decreased by 3.9% and 25.4%, respectively. However, the foam volume of the SLX foam increased by 6.3% and its foam drainage half-life reduced by 65.6%. It was quite clear that high temperature had few influences on the foamability, but had poor effect on the foam stability, particularly for the SLX foam. Viscosity measurement showed that the SLX solution viscosity decreased from 28 mPa s to 5.3 mPa s after aged for 90 days. This result indicated that the XG degraded due to exposure in high temperature and high salinity environment for a long time. The degradation would cause the molecular chain of the XG to rupture and shorten.[38] The steric hindrance at the gas/

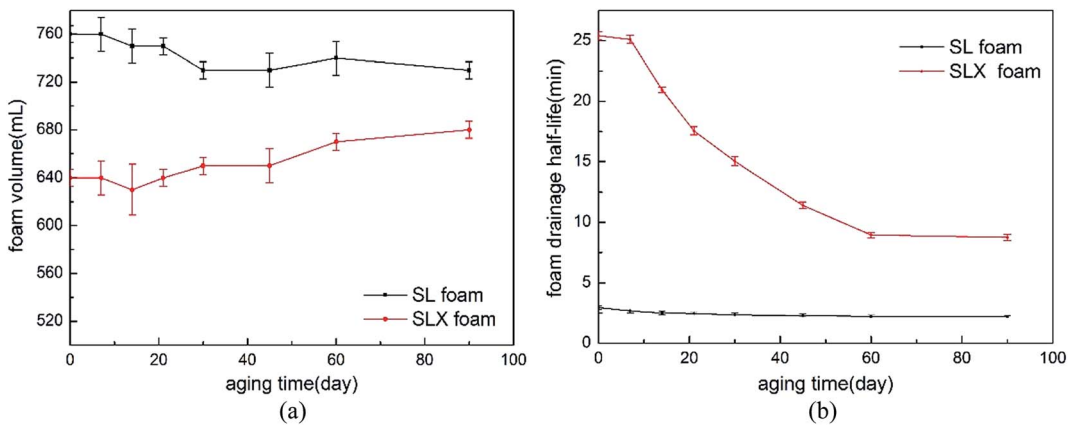

Fig. 2 Foam properties for aged SL foam and aged SLX foam generated by aged surfactant solution and aged polymer–surfactant solution, respectively (90 °C). (a) Foam volume, (b) foam drainage half-life. The time when the aging test just began was the base line of time ($t = 0$).

Published on 25 February 2015. Downloaded by Michigan State University on 29/01/2016 16:18:21.

water interface and the foam film strength weakened accordingly. Nevertheless, the degraded XG molecules still had some stabilization effect on foam, so the foam drainage half-life of the aged SLX foam was four times as long as that of the fresh SL foam. Additionally, the decreased solution viscosity reduced the viscous resistance of foaming, hence the foam volume of the SLX foam increased during aging.

The microstructures of different foams are shown in Fig. 3. The fresh SL foam film seemed like a thin rod which formed by the accumulated flake materials (Fig. 3(b)). The flake materials were SDS and LC that gathered by electrostatic force (SDS and LC could ionize anions and cations in the neutral solution, respectively) and van der Waals force. The rod structure was small in size and weak in strength, which caused the SL foam film easy to rupture. Fig. 3(c) shows a dense network microstructure of the fresh SLX foam. Bubbles which had similar size uniformly distributed among foam films that developed by surfactants and XG. With the combination of electrostatic force and hydrophobic association, the semi-rigid XG macromolecules wrapped the small surfactant molecules to form a multilayer complex (Fig. 3(d)). This made the foam film thick and solid both in horizontal and vertical directions. Thus, the fresh SLX foam had good stability. After aged at 90 °C for 45 days, the SLX foam still kept its three-dimensional network structure (Fig. 3(e)). But when the structure (focused on the foam film) was magnified 5000 times (Fig. 3(f)), lots of cavities appeared in the foam films, the XG-surfactant complex seemed vulnerable, and some separate flake structures could be recognized. This visible information was consistent with the preceding viscosity measurement result. It demonstrated once again that the XG molecular chain was broken during aging. However, the foam film strength and the bubble size distribution of the aged SLX foam improved considerably compared to the fresh SL foam, which resulted better foam stability.

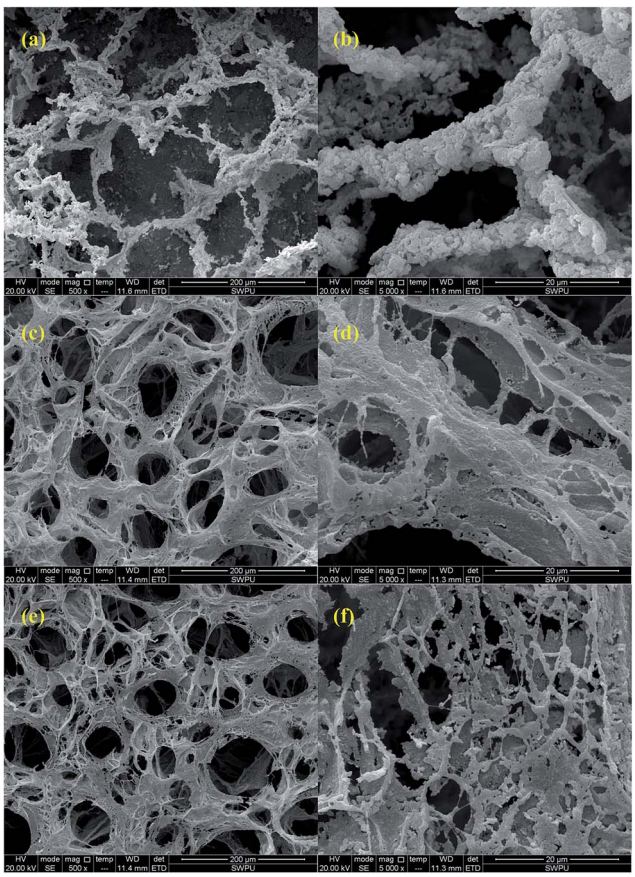

Fig. 3 Microstructures of different foams: (a) and (b) the fresh SL foam which was generate by the fresh surfactant solution, (c) and (d) the fresh SLX foam which was generated by the fresh polymer–surfactant solution, and (e) and (f) the aged SLX foam which was generated by the aged polymer–surfactant solution. Images (a), (c) and (e) were magnified 500 times, while (b), (d) and (f) were magnified 5000 times which focused on the foam film.

3.2. Oil tolerance of foam

Different volumes of crude oil were added to the SL foam solution or the SLX foam solution before foaming to identify the oil tolerance of corresponding foam. Fig. 4 demonstrates that the mixture of foam solution and crude oil can generate abundant foam. According to Fig. 5, for the SL foam, when the oil content was not more than 20%, the foam volume in the presence of oil was similar to in the absence of oil, and the foam drainage half-life in the presence of oil was even longer than in the absence of oil (the foam drainage half-life prolonged with increasing oil content). For the SLX foam, when the oil content was not more than 60%, the foam volume was almost constant as the oil amount increased. When the oil content was not more than 20%, the foam drainage half-life in the presence of oil was also longer than in the absence of oil. The foam in the presence of 10% oil had the longest drainage half-life. Fig. 5(b) displayed that, when the oil content increased from 0% to 40% (60%), the stability of the SL foam and the SLX foam reduced by 22.5% (53.6%) and 12.5% (43.1%), respectively. It indicated that the XG could alleviate the foam thinning in the presence of high oil amount. Similar result was observed in Chen *et al.*[39] recent work. Their experiments showed that polymer could increase the oil tolerance of foam.

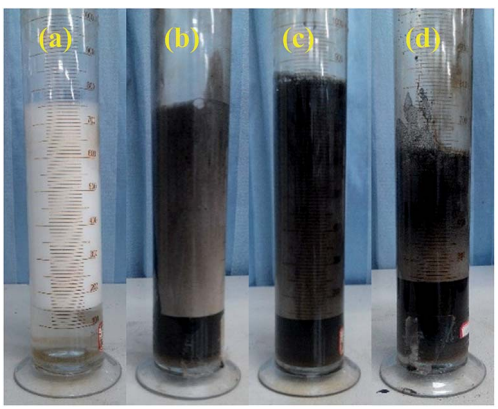

Fig. 4 Foam appearances for SL solution with different volume of crude oil: (a) pure SL, (b) SL + 10% oil, (c) SL + 20% oil, and (d) SL + 40% oil (images were taken after each foam had produced for 5 minutes at 90 °C).

 This journal is © The Royal Society of Chemistry 2015

Published on 25 February 2015. Downloaded by Michigan State University on 29/01/2016 16:18:21.

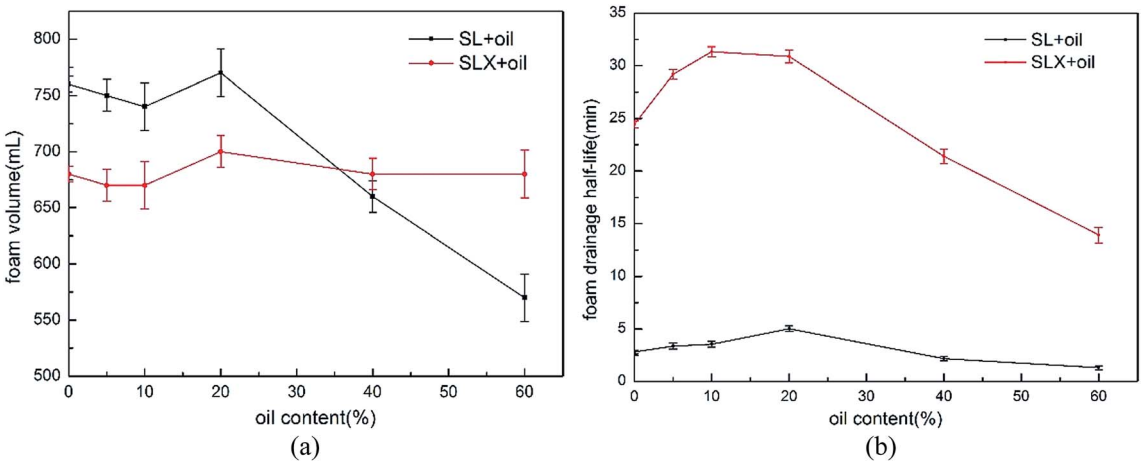

Fig. 5 (a) Foam volume and (b) foam drainage half-life for SL solution/SLX solution with different volumes of crude oil (90 °C).

Fig. 6 exhibits the microphotographs of foams in the presence of different crude oil content that obtained with stereoscopic microscope. When the oil content was 5% (Fig. 6(a)), the oil dispersed in the foam film in the form of stable O/W emulsion droplets. These droplets could increase the viscosity and strength of the foam film, build a stable pseudo-emulsion film, and eventually enhance the foam stability. The stabilization effect of emulsified oil on foam had also been reported earlier by Koczo *et al.*[40] He discussed that, if the pseudo-emulsion film was stable, the emulsified oil drops in the Plateau borders could inhibit the liquid drainage. When the oil content enlarged to 10% (Fig. 6(b)), the oil still existed in the form of O/W emulsion droplets. Nevertheless, their size decreased and number increased. Smaller O/W emulsion droplets which had better stability made the pseudo-emulsion film much more stable. More O/W emulsion droplets further enhanced the viscosity and strength of the foam film. Therefore, the drainage half-life prolonged from 24.5 minutes (with no oil) to 31.3 minutes. However, when the oil content enlarged to 20% (Fig. 6(c)), the appearance of the oil in the foam film changed. It existed not only in the form of O/W emulsion droplets (these droplets could be clearly seen at the foam film border), but also in the form of W/O emulsion droplets (these droplets had highlighted water in the center). Although the W/O emulsion had better stability and viscosity than the O/W emulsion, it took the foam solution which had high surface activity as internal phase, caused the surface activity of the entire system to reduce. As a result, the drainage half-life slightly dropped down to 30.9 minutes. When the oil content further enlarged to 60% (Fig. 6(d)), the light transmission of the foam film sharply declined due to the packed oil droplets. On the one hand, the emergence of these oil droplets resulted in an enormous amount of surfactant molecules diffusing towards them. Then, the quantity of surfactant molecules at the gas/water interface reduced,[30,34] likely weakening the foam film strength and Marangoni effect. On the other hand, the emergence of these oil droplets amplified the oil/water interfacial area. It caused the surfactant concentration at the oil/water interface to decrease, and thus the pseudo-emulsion film stability to reduce. Once the pseudo-emulsion film ruptured, the oil would enter into the gas/water interface, and eventually induced the foam film to rupture. Therefore, the drainage half-life shortened to 13.9 minutes.

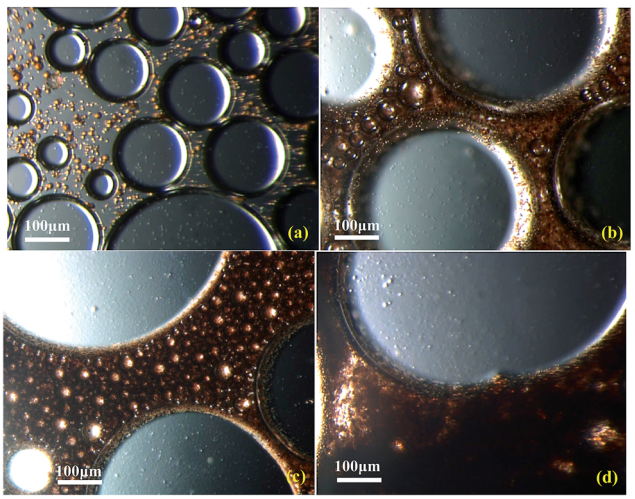

Fig. 6 Microphotographs of SLX solution with different volume of crude oil: (a) SLX + 5% oil, (b) SLX + 10% oil, (c) SLX + 20% oil, and (d) SLX + 40% oil. The brown part in the foam film was crude oil, the others were foam solutions (the microphotographs were magnified 200 times).

The above experiments revealed that the existing form and content of oil in the foam film had important influence on the stability of pseudo-emulsion film, and dominated the stability of foam with oil. Meanwhile, the abundant complicated molecules such as resin, asphaltene and paraffin in the studied crude oil also contributed to the high oil tolerance of the foams. As the literature reported,[28,31,41,42] these complicated molecules made crude oil difficult to solubilize in surfactant micelles to destroy their activity and could give the formed emulsions better stability. In addition, the microscope images illustrated that, with increasing crude oil content, the foam size continually enlarged, which was inconsistent with the change of the drainage half-life. This interesting response

Published on 25 February 2015. Downloaded by Michigan State University on 29/01/2016 16:18:21.

suggested that the foam size was not crucial for foam stability in the presence of oil.

3.3. Core flooding experiments

Core flooding experiments were carried out at temperature of 90 °C and pressure of 13.7 MPa. Experiment results are shown in Fig. 7 and Table 5.

Fig. 7 illustrates the oil recovery and water cut for the four core flooding experiments investigated. Comparison of core 1 and core 2 found that, even with similar water flooding recovery and the same liquid chemical agent (the injected volume of the core 1 was only one-third of the core 2), the former acquired more incremental oil recovery, higher pressure drop and lower water cut due to the gas–liquid co-injection (Table 5). This confirmed that air and foam solution co-injection was able to produce stable foams in the presence of crude oil. The foams in the core would generate a Jamin effect, triggering stronger mobility control and more effective pressure build-up than single liquid displacement agent. Moreover, the low price of gas made foam flooding more economically attractive over surfactant flooding and surfactant/polymer flooding.

With regard to cores 1, 3 and 4, because of their close core properties and the same water injection rate, their oil recovery profile and water cut profile during the water flooding period were similar, and their oil saturations after water flooding were all around 37%. However, after foam had been injected, the differences were observed. For the core 1, once the fresh SLX foam entered into the porous media, oil was produced at a high rate, and a drop was presented in the water cut profile immediately. It indicated that the fresh SLX foam generated good mobility control in the high permeability regions due to its high viscosity and strength. Then, the oil that swept or not swept by the previous injected water could be displaced. Finally, the fresh SLX foam (0.4 PV) yielded an incremental oil recovery of 18.18%. During subsequent water flooding, the fresh SLX foam still exerted some flow resistance in the high permeability regions, enabling the injected water sweep the remaining oil enrichment areas (mainly in the low permeability regions) and recover additional oil. Until 1.0 PV of water was injected, the water cut reached 98%, and the cumulative oil recovery was up to 78.92%. For the core 3, interesting responses were seen: (I) oil recovery and water cut appeared evidently improvement almost when 0.4 PV of the fresh SL foam had been injected; (II) water cut rose rapidly during subsequent water flooding, and went up to 96% only after 0.3 PV of water was injected. These responses reflected that the mobility control capability of the fresh SL foam was reduced compared to the fresh SLX foam. Moreover, owing to the weaker foam strength, more injected volume was needed for the SL foam to build sufficient flow resistance in the high permeability regions. Thus, the pressure drop only reached to 1.19 MPa at the end of the SL foam flooding, which was even poorer than that of the SLX solution flooding. For the core 4, the responses obtained in the aged SLX foam flooding were slow oil

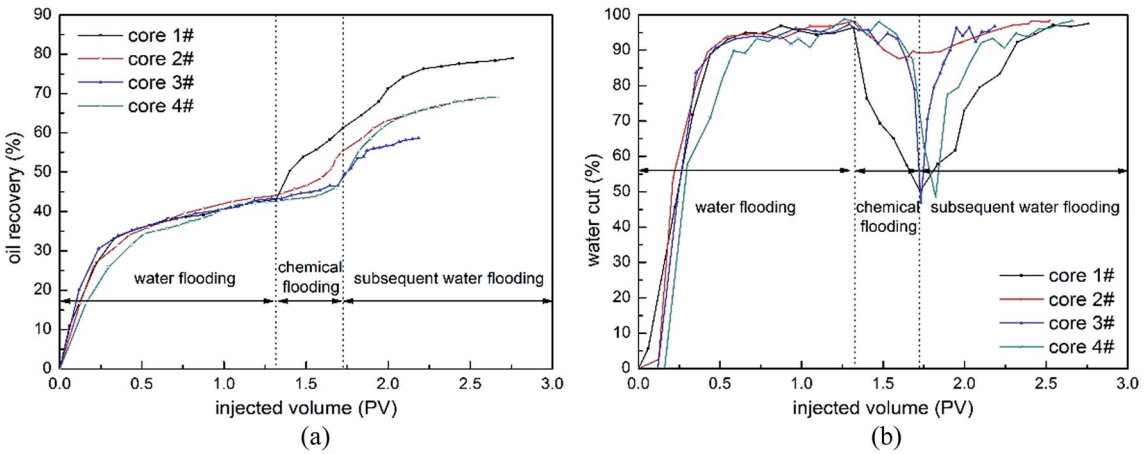

Fig. 7 (a) Oil recovery profile and (b) water cut profile for core flooding experiments performed in this study. Each profile started with water flooding followed by chemical flooding (foam flooding or surfactant/polymer flooding) and then subsequent water flooding. The time when the first water flooding just began was the base line of time ($t = 0$).

Table 5 Summary of oil recovery and pressure drop during oil displacement

Core number	Chemical displacement agent	Water flooding recovery (%)	Incremental oil recovery (%)	Total recovery (%)	Max pressure drop of chemical flooding (MPa)
1#	Fresh SLX foam	43.17	35.75	78.92	2.79
2#	Fresh SLX solution	44.06	24.41	68.47	1.76
3#	Fresh SL foam	43.31	15.35	58.66	1.19
4#	Aged SLX foam	42.74	26.45	69.19	1.96

 This journal is © The Royal Society of Chemistry 2015

Published on 25 February 2015. Downloaded by Michigan State University on 29/01/2016 16:18:21.

increment and tardy water cut drop. The high temperature aging also weakened the strength and stability of SLX foam in the porous media. However, the aged SLX foam had considerable improvement in mobility control compared to the fresh SL foam, which corresponded to the more oil recovery and the higher pressure drop.

The core flooding work could not represent what happens in the reservoir and there is a need to better understand foam break-up and regeneration, surfactant adsorption and other factors in a reservoir situation.

4. Conclusion

1. The SL foam (surfactant foam) that formed by the mixture of sodium dodecyl sulfate and imidazoline amphoteric surfactant had excellent high temperature tolerance. Xanthan gum could enhance its foam stability and form SLX foam (polymer–surfactant foam) with good high temperature tolerance.

2. The microstructures of the SL foam film and the SLX foam film were a thin rod and a thick multilayer complex, respectively. The latter was stronger and more stable both in a cylinder and in a flooded core, even when exposed to high temperature for a long time.

3. Bulk foam tests and core flooding experiments verified that stable foam (both surfactant foam and polymer–surfactant foam) could be generated in the presence of oil.

4. Both the SL foam and the SLX foam had outstanding oil tolerance. Within a certain oil content, the foam volume in the presence of oil was similar to in the absence of oil, whereas the foam drainage half-life in the presence of oil was even longer than in the absence of oil and it could prolong as the oil amount increased. The XG could alleviate the drainage rate of foam in the presence of high oil content. Further studies are needed for a full explanation.

5. The existing form and content of oil in the foam film were the key factors that controlled the oil tolerance of foam. A few small O/W emulsion droplets were favorable for foam stability in the presence of oil.

6. Air and foam solution co-injection could generate stable foam in water-flooded core and additional oil recovery was achieved by the foam. The SLX foam possessed better oil displacement efficiency than the SLX solution and the SL foam. Even aged at 90 °C for 90 days, the aged SLX foam could still yield more oil recovery than the fresh SL foam.

Acknowledgements

The authors gratefully acknowledge the special fund of China's central government for the development of local colleges and universities—the project of national first-level discipline in Oil and Gas Engineering.

Notes and references

1 Å. Haugen, N. Mani, S. Svenningsen, B. Brattekås, A. Graue, G. Ersland and M. A. Fernø, *Transp. Porous Media*, 2014, 1–23.
2 M. Namdar Zanganeh and W. Rossen, *SPE Reservoir Eval. Eng.*, 2013, **16**, 51–59.
3 R. Farajzadeh, A. Andrianov and P. Zitha, *Ind. Eng. Chem. Res.*, 2009, **49**, 1910–1919.
4 W. R. Rossen, *Surfactant Sci. Ser.*, 1996, 413–464.
5 A. Maestro, E. Rio, W. Drenckhan, D. Langevin and A. Salonen, *Soft Matter*, 2014, **10**, 6975–6983.
6 R. Petkova, S. Tcholakova and N. D. Denkov, *Langmuir*, 2012, **28**, 4996–5009.
7 S. Zhang, Q. Lan, Q. Liu, J. Xu and D. Sun, *Colloids Surf., A*, 2008, **317**, 406–413.
8 R. G. Alargova, D. S. Warhadpande, V. N. Paunov and O. D. Velev, *Langmuir*, 2004, **20**, 10371–10374.
9 S. Li, Z. Li and B. Li, *J. Pet. Sci. Eng.*, 2014, **118**, 88–98.
10 X. Liang, M. H. Xiang, Y. Yang, Q. H. Chen and Z. R. Shu, *Appl. Mech. Mater.*, 2011, **71**, 2163–2168.
11 S. Li, Z. Li and B. Li, *J. Pet. Sci. Eng.*, 2011, **78**, 567–574.
12 F. Friedmann, W. H. Chen and P. A. Gauglitz, *SPE Reservoir Eng.*, 1991, **6**, 37–45.
13 H. P. Angstadt and H. Tsao, *SPE Reservoir Eng.*, 1987, **2**, 613–618.
14 R. M. Muruganathan, R. Krastev, H. Müller and H. Möhwald, *Langmuir*, 2006, **22**, 7981–7985.
15 P. N. Quoc, P. L. Zitha and P. K. Currie, *J. Colloid Interface Sci.*, 2002, **248**, 467–476.
16 R. Farajzadeh, A. Andrianov, H. Bruining and P. L. Zitha, *Ind. Eng. Chem. Res.*, 2009, **48**, 4542–4552.
17 S. I. Kam, W. W. Frenier, S. N. Davies and W. R. Rossen, *SPE 82266, SPE European Formation Damage Conference*, The Hague, Netherlands, 13–14 May 2003.
18 Y. Chen, A. S. Elhag, B. M. Poon, L. Cui, K. Ma, S. Y. Liao, A. Omar, A. Worthen, G. J. Hirasaki and Q. P. Nguyen, *SPE 154222, SPE Improved Oil Recovery Symposium*, Tulsa, Oklahoma, USA, 14–18 April 2012.
19 M. Simjoo, Y. Dong, A. Andrianov, M. Talanana and P. L. Zitha, *SPE 155633, SPE EOR Conference at Oil and Gas West Asia*, Muscat, Oman, 16–18 April 2012.
20 A. K. Vikingstad and M. G. Aarra, *J. Pet. Sci. Eng.*, 2009, **65**, 105–111.
21 L. Arnaudov, N. D. Denkov, I. Surcheva, P. Durbut, G. Broze and A. Mehreteab, *Langmuir*, 2001, **17**, 6999–7010.
22 A. Hadjiiski, S. Tcholakova, N. D. Denkov, P. Durbut, G. Broze and A. Mehreteab, *Langmuir*, 2001, **17**, 7011–7021.
23 T. J. Myers and C. J. Radke, *Ind. Eng. Chem. Res.*, 2000, **39**, 2725–2741.
24 A. D. Nikolov, D. T. Wasan, D. W. Huang and D. A. Edwards, *SPE 15443, SPE Annual Technical Conference and Exhibition*, New Orleans, Louisiana, 5–8 October 1986.
25 R. F. Li, G. J. Hirasaki, C. A. Miller and S. K. Masalmeh, *SPE 14146, SPE International Symposium on Oilfield Chemistry*, The Woodlands, Texas, USA, 11–13 April 2011.
26 A. K. Vikingstad, PhD dissertation, The University of Bergen, 2006.
27 K. Mannhardt, J. J. Novosad and L. L. Schramm, *SPE 39681, SPE/DOE Improved Oil Recovery Symposium*, Tulsa, Oklahoma, 19–22 April 1998.

Published on 25 February 2015. Downloaded by Michigan State University on 29/01/2016 16:18:21.

28 A. Andrianov, R. Farajzadeh, M. Mahmoodi Nick, M. Talanana and P. Zitha, *Ind. Eng. Chem. Res.*, 2012, **51**, 2214–2226.
29 H. Cubillos, J. Montes, C. Prieto and P. Romero, *SPE 152113, SPE Improved Oil Recovery Symposium*, Tulsa, Oklahoma, USA, 14–18 April 2012.
30 M. Simjoo, T. Rezaei, A. Andrianov and P. Zitha, *Colloids Surf., A*, 2013, **438**, 148–158.
31 A. K. Vikingstad, A. Skauge, H. H. O. Iland and M. Aarra, *Colloids Surf., A*, 2005, **260**, 189–198.
32 R. Aveyard, B. P. Binks, P. Fletcher, T. G. Peck and C. E. Rutherford, *Colloids Surf., A*, 1994, **48**, 93–120.
33 J. Lee, A. Nikolov and D. Wasan, *Ind. Eng. Chem. Res.*, 2013, **52**, 66–72.
34 R. Farajzadeh, A. Andrianov, R. Krastev, G. J. Hirasaki and W. R. Rossen, *Adv. Colloid Interface Sci.*, 2012, **183–184**, 1–13.
35 D. J. Manlowe and C. J. Radke, *SPE Reservoir Eng.*, 1990, **5**, 495–502.
36 Q. Sang, Y. Li, L. Yu, Z. Li and M. Dong, *Fuel*, 2014, **136**, 295–306.
37 B. Jean, L. Lee, B. Cabane and V. Bergeron, *Langmuir*, 2008, **25**, 3966–3971.
38 F. Lambert and M. Rinaudo, *Polymer*, 1985, **26**, 1549–1553.
39 S. Y. Chen, G. Q. Jian, Q. F. Hou, S. L. Gao, Y. S. Luo, Y. Y. Zhu and W. J. Li, *Int. J. Oil, Gas Coal Technol.*, 2013, **6**, 675–688.
40 K. Koczo, L. A. Lobo and D. T. Wasan, *J. Colloid Interface Sci.*, 1992, **150**, 492–506.
41 N. D. Denkov, *Langmuir*, 2004, **20**, 9463–9505.
42 F. E. Suffridge, K. T. Raterman and G. C. Russell, *SPE 19691, SPE Annual Technical Conference and Exhibition*, San Antonio, Texas, 8–11 October 1989.

 This journal is © The Royal Society of Chemistry 2015